INTERNATIONAL JOURNAL OF HYDROGEN ENERGY 45 (2020) 25002–25012

Available online at www.sciencedirect.com

ScienceDirect

journal homepage: www.elsevier.com/locate/he

Enhanced thermodynamic properties of $ZrNiH_3$ by substitution with transition metals (V, Ti, Fe, Mn and Cr)

M. Rkhis [a,**], A. Alaoui-Belghiti [a], S. Laasri [a,*], S. Touhtouh [a], A. Hajjaji [a], E.K. Hlil [b], M. Bououdina [c], K. Zaidat [d], S. Obbade [e]

[a] Laboratoire des Sciences de l'Ingénieur pour l'Energie, Ecole Nationale des Sciences Appliquées d'El Jadida, BP 1166, EL Jadida Plateau, 24002, Morocco

[b] Institut Néel, CNRS et Université Grenoble Alpes, BP 166, Grenoble, 38042, France

[c] Department of Physics, College of Science, University of Bahrain, PO Box, 32038, Southern Governorate, Bahrain

[d] University of Grenoble, SIMAP-EPM, BP 75, Saint Martin d'Heres Cedex, 38402, France

[e] LEPMI UMR 5279, Grenoble INP, Université Grenoble Alpes, BP 75, Saint-Martin d'Hères Cedex, 38402, France

HIGHLIGHTS

- The pure $ZrNiH_3$ presents high stability and decomposition temperature.
- The stability reduces when $ZrNiH_3$ is substituted with transition metals.
- The electronic structure reveals the metallic character of $Zr_{1-x}TM_xNiH_3$ hydrides.

ARTICLE INFO

Article history:
Received 7 March 2020
Received in revised form
16 June 2020
Accepted 22 June 2020
Available online 17 August 2020

Keywords:
Ab initio calculations
$ZrNiH_3$
Transition metal
Hydrogen storage
Thermodynamic properties

ABSTRACT

First-principles calculations based on Plane-Wave Self-Consistent Field (PWSCF) method, implemented in quantum espresso program, have been performed on $ZrNiH_3$ substituted with transition metals (V, Ti, Fe, Mn, and Cr). The study aims to investigate the heat of formation in terms of material stability and desorption temperature. It is found that the substitution by transition metals, results in a significant enhancement in the thermodynamic properties accompanied by an increase of the volumetric and gravimetric hydrogen storage capacities. In addition, the obtained values of heat of formation and desorption temperature corroborate with that required by the U.S. Department of Energy (DOE) for stability and volumetric capacity criteria. Moreover, Mn and Fe elements are found to present the lowest substituting content (34%) to obtain optimum hydrogen storage characteristics (enthalpy of formation of - 40 kJ/mol.H_2, decomposition temperature of 300 K and volumetric capacity of 134 g.H_2/l), without affecting the electronic structure and the metallic character of $ZrNiH_3$.

* Corresponding author.
** Corresponding author.
E-mail addresses: mourad.rk04@gmail.com (M. Rkhis), laasri.s@ucd.ac.ma, laasrisaid@yahoo.fr (S. Laasri).
https://doi.org/10.1016/j.ijhydene.2020.06.213

Introduction

For a few decades, scientists have been focusing on renewable energies as an alternative source to prevent global warming and emission of greenhouse gases [1]. Among the subjects of concern, the use of hydrogen as an energy source for the future economy becomes of great importance [2]. Hydrogen possesses outstanding properties and can be transformed into a promising clean fuel. In fact, it is the most abundant element in the universe with the highest energy content compared to any other fuel. Unlike oil or natural gas, hydrogen is non-toxic. Only water vapor is released into the environment during its energy conversion [3]. However, the storage and the transport of hydrogen remain very challenging that limits its use and its large-scale commercialization [4].

Generally, hydrogen is usually stored in gaseous form at high pressure as well as liquid at low temperature [5]. Both techniques demonstrate several disadvantages that do not meet the future goals for a hydrogen economy, such as safety under high pressure and the cost of the energy requested for hydrogen liquefaction. Fortunately, extensive researches have focused on the storage in solid form, either by adsorption on materials having a large specific surface such as porous systems (carbon nanostructures, zeolites, and metallo-organic frameworks MOFs) or by absorption into intermetallic hydrides which demonstrated a great potential to store hydrogen in large quantities in a quite secure and reversible manner [6–9].

Intermetallic hydrides have been used in many applications, one of the most essential is nickel metal hydride (Ni-MH) rechargeable batteries, which are widely commercialized as power sources for hybrid electric, fuel cell vehicles as well portable devices [10–13]. Ni-MH batteries are known to have a compact size, long lifetime, high-rate capability, and environmental friendliness [14–16]. However, they exhibit low storage energy density compared to lithium-ion batteries. Nevertheless, lithium-ion batteries are known to have a severe problem concerning safety since they use a flammable organic electrolyte [17,18]. For this purpose, it is meaningful to develop new negative electrode active materials with increasing energy density and safety. Zirconium-based alloys such as AB-type ZrNi are very promising materials for solid-state hydrogen storage [19–26]. This system absorbs three hydrogen atoms per formula unit, forming $ZrNiH_3$ as an attractive negative electrode active material for Ni-MH batteries because it has a theoretical capacity of about 500 mAh/g, thats is higher than that of AB_3- or AB_5-type rare-earth-based commercial alloys (300 mAh/g) [27–29]. However, Matsuyama et al. [30] reported that the initial discharge capacity of $ZrNiH_3$ was found much smaller than the theoretical capacity, reaching only 320 mAh/g at 333 K, because $ZrNiH_3$ was too stable to release the total amount of the absorbed hydrogen ($\Delta H = -68.8$ kJ/mol.H_2) [31,32]. Its high stability and high dissociation temperature of 547 K essentially limits its application for hydrogen storage on a large scale [33]. Consequently, further researches are necessary in order to destabilize $ZrNiH_3$ by enhancing its hydrogen release or discharge capacity.

Many attempts have been devoted to investigate this material experimentally and theoretically in order to improve its hydrogen storage properties. In this regard, some studies [33,34] reported the effect of single substitution of Zr with transition metals such as 4d Nb with a low content of 10% or using 3d Ti with a high content ranging from 5% to 50%. It was found that when Zr is replaced by 10% of Nb, $Zr_{0.9}Nb_{0.1}NiH_3$ exhibits the best results, with an ideal heat of formation ($\Delta H = -39.9$ kJ/mol.H_2) and desorption temperature ($T_{des} = 305.77$ K) without affecting its gravimetric capacity.

The aim of this study is to assess the effect of substituting Zr by 3d transition metals (TM = V, Ti, Fe, Mn, and Cr) in order to tune $ZrNiH_3$ strong hybridization and therefore reduce its high stability and desorption temperature. All calculations are carried out in the framework of density functional theory (DFT) [35] with Plane-Wave Self-Consistent Field method (PWSCF) implemented in quantum espresso program [36]. The formation energy and the corresponding hydrogen storage thermodynamic properties of the substituted system $Zr_{1-x}TM_xNiH_3$ (x = 0.25 and 0.50) are explicitly computed. Particular attention has been devoted to the hybridization between orbitals using density of state techniques.

Models and computational details

In order to determine the different properties of the studies compounds, ab-initio calculations have been performed based on density functional theory approach [35], where the exchange and correlation energy corrections are included through a generalized gradient approximation (GGA) [37] with Plane-Wave Self-Consistent Field method (PWSCF), implemented in the quantum espresso code [36]. All pseudopotentials are constructed using the ultrasoft pseudopotential method [38] with a cutoff kinetic energy of 600 eV, and the k-point grids for the whole Brillouin zone are sited to be 9 × 3 × 8, usually giving a good convergence of the total energy within 1 meV/atom. The atomic positions and the cell parameters are fully optimized by minimizing the Hellmann-Feynman [39] stresses and forces without any symmetry constraint.

$ZrNiH_3$ crystallizes in an orthorhombic structure, with a space group Cmcm (N° 63) and lattice parameters a = 3.53 Å, b = 10.48 Å and c = 4.30 Å [22,40]. In this structure, there are 4 formula units (f.u.) per cell, where Zr and Ni atoms occupy the Wyckoff positions 4c (0; 0.140; 0.25) and 4c (0; 0.430; 0.25) respectively. The H atoms occupy two types of interstitial sites 4c (0; 0.956; 0.25) and 8f (0; 0.298; 0.507). For the case of single substitution (25%), one Zr atom is substituted by 1 atom of either V, Ti, Fe, Mn, or Cr ($Zr_{0.75}V_{0.25}NiH_3$, $Zr_{0.75}Ti_{0.25}NiH_3$, $Zr_{0.75}Fe_{0.25}NiH_3$, $Zr_{0.75}Mn_{0.25}NiH_3$, $Zr_{0.75}Cr_{0.25}NiH_3$). For double substitution, two Zr atoms (50%) are substituted by two atoms of either V, Ti, Fe, Mn, or Cr ($Zr_{0.5}V_{0.5}NiH_3$, $Zr_{0.5}Ti_{0.5}NiH_3$, $Zr_{0.5}Fe_{0.5}NiH_3$, $Zr_{0.5}Mn_{0.5}NiH_3$, $Zr_{0.5}Cr_{0.5}NiH_3$). The different systems are presented in Fig. 1.

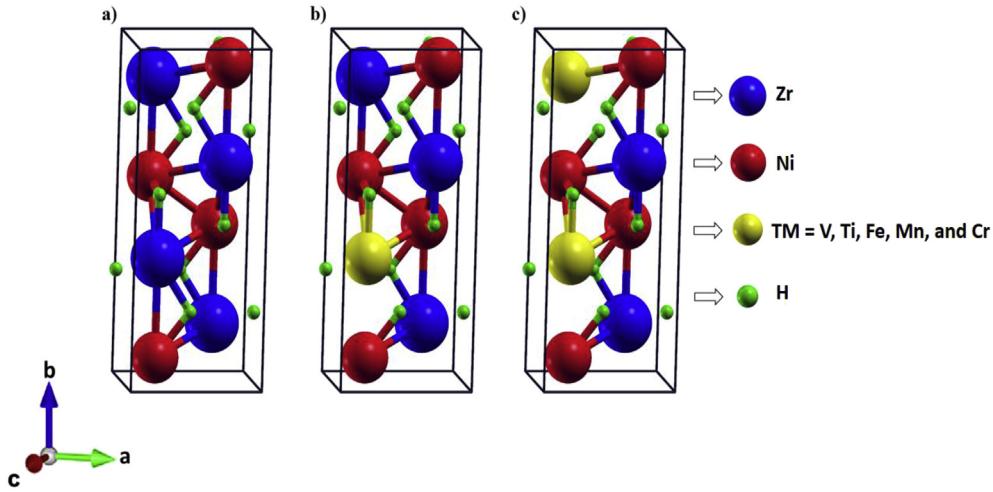

Fig. 1 – Crystal structure of (a) $ZrNiH_3$, (b) $Zr_{0.75}TM_{0.25}NiH_3$ and (c) $Zr_{0.5}TM_{0.5}NiH_3$ (TM = V, Ti, Fe, Mn, and Cr).

Results and discussion

Equilibrium structure and storage capacity

Before studying the thermodynamic properties in terms of enthalpy of formation and desorption temperature of $Zr_{1-x}TM_xNiH_3$ system (TM = V, Ti, Fe, Mn, and Cr; x = 0, 0.25 and 0.50), the geometries have been completely relaxed. Indeed, because of the different values of the atomic radius in the studied compositions, the substitution breaks the symmetry and results in different lattice parameters and therefore creates changes in the periodicity of the crystal. For this reason, the lattice parameters for which the system will be more stable has been determined. This has been carried out by varying the volume of the unit cell around its experimental value. Table 1 summarizes the optimized lattice parameters and unit cell volume of all compositions.

According to the obtained results in Fig. 2, for all compounds the lattice parameters a and b decrease with increasing the content x of the transition metals TM, whereas c slightly decreases and consequently V decreases. Similar observation was reported by Matsuyama et al. [33] for $Zr_{1-x}Ti_xNi$ system ($0.05 \leq x \leq 0.5$). Moreover, the linear relationship between the unit cell volume V and the content x of the TM agrees with Vegard's law [41]. On the other hand, it can be concluded from Table 1 and Fig. 3 that, the incorporation of transition metals (V, Ti, Fe, Mn and Cr) with contents of 25% and 50%, generates a slight variation of the lattice parameters leading to the contraction of the unit cell volume. Consequently, this change causes an increase in volumetric capacity from 125 g.H_2/l (pure $ZrNiH_3$) to 130 up to 135 g.H_2/l for the system with x = 0.25 and 135 up to 143 g.H_2/l for the system with x = 0.5. Also, it induces an increase in the gravimetric capacity from 1.97 to 2.1 wt% and 2.3 wt% for x = 0.25 and 0.5, respectively.

Table 1 – Optimized lattice parameters, volumes, gravimetric and volumetric capacities of $Zr_{1-x}TM_xNiH_3$ (TM = V, Ti, Fe, Mn, and Cr).

System	Parameters (Å)			Volume (Å^3)	Gravimetric capacity (wt.%)	Volumetric capacity (g.H_2/l)
	a	b	c			
$ZrNiH_3$ This study	3.55321	10.46591	4.29559	159.74327	1.977	125.726
$ZrNiH_3$ [22,40]	3.53	10.48	4.30	159.07		
$Zr_{0.75}V_{0.25}NiH_3$	3.49614	10.23148	4.24572	151.87293	2.116	132.241
$Zr_{0.5}V_{0.5}NiH_3$	3.41339	10.01696	4.21048	143.96412	2.276	139.506
$Zr_{0.75}Ti_{0.25}NiH_3$ This study	3.50130	10.34276	4.27200	154.70287	2.127	129.822
$Zr_{0.75}Ti_{0.25}NiH_3$ [33]	3.4	10.18	4.24	147.75		
$Zr_{0.5}Ti_{0.5}NiH_3$ This study	3.43202	10.23333	4.25482	149.43403	2.303	134.399
$Zr_{0.5}Ti_{0.5}NiH_3$ [33]	3.228	10.14	4.25	139.11		
$Zr_{0.75}Fe_{0.25}NIH_3$	3.47104	10.11327	4.26471	149.70692	2.098	134.154
$Zr_{0.5}Fe_{0.5}NiH_3$	3.34578	9.86384	4.23686	139.8265	2.235	143.634
$Zr_{0.75}Mn_{0.5}NIH_3$	3.49347	10.11444	4.23644	149.69293	2.101	134.167
$Zr_{0.5}Mn_{0.5}NiH_3$	3.33866	9.90017	4.23919	140.11959	2.243	143.333
$Zr_{0.25}Cr_{0.75}NiH_3$	3.48353	10.17151	4.24727	150.49294	2.112	133.454
$Zr_{0.5}Cr_{0.5}NiH_3$	3.35412	9.95240	4.23533	141.38251	2.267	142.053

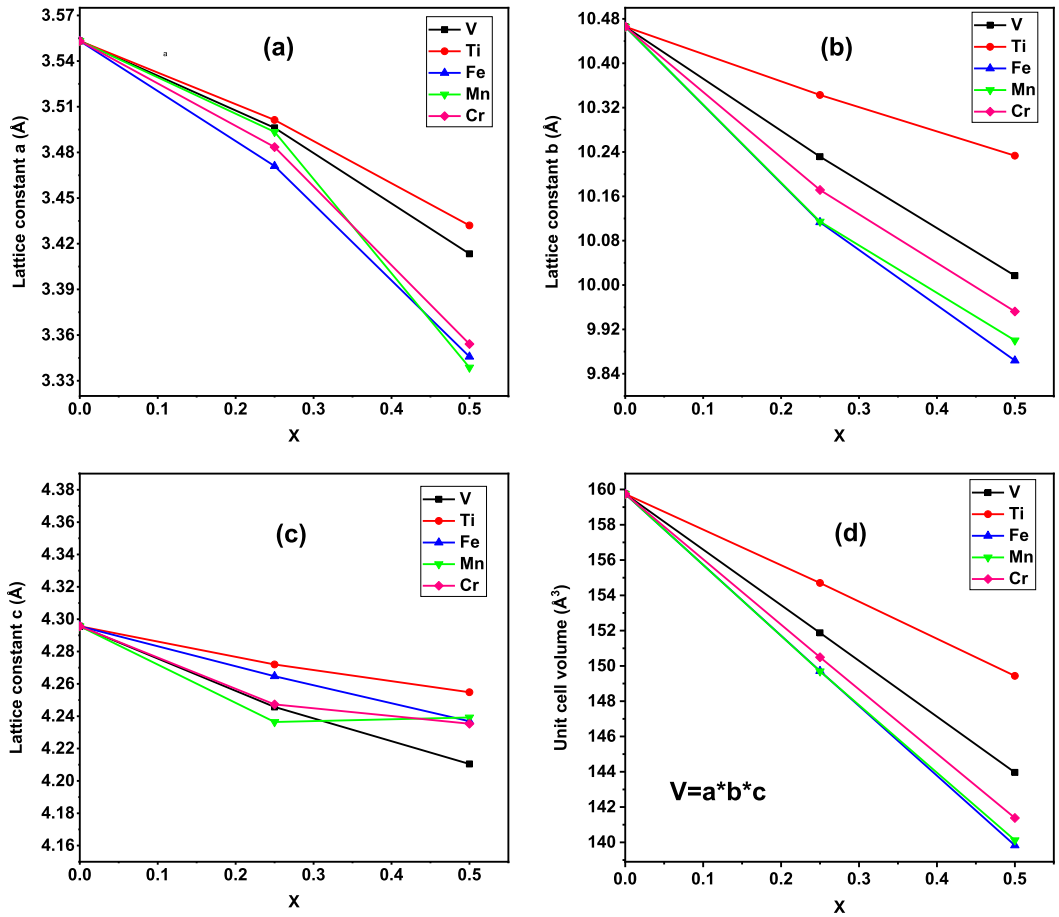

Fig. 2 – Variation of lattice parameters (a, b and c) and unit cell volume with TM content of $Zr_{1-x}TM_xNiH_3$ (TM = V, Ti, Fe, Mn, and Cr). (a) a, (b) b, (c) c and (d) unit cell volume.

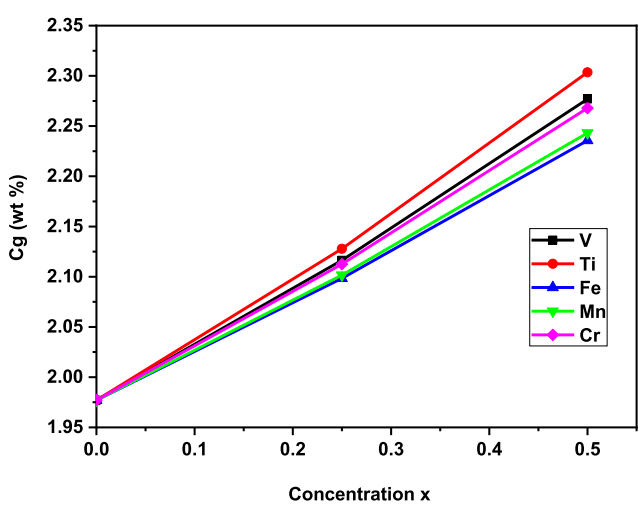

Fig. 3 – Gravimetric capacity of $Zr_{1-x}TM_xNiH_3$ according to the content x of substitution.

Stability of the intermetallic hydrides and enthalpy of formation

The enthalpy of formation ΔH has been determined to study the dehydrogenation properties and the phase stability of $ZrNiH_3$ and $Zr_{1-x}TM_xNiH_3$ hydrides. Indeed, it is the most important thermodynamic parameter used to classify and characterize materials for hydrogen storage applications. It is given by Hess's law as the difference between the total energies of products and reactants:

$$\Delta H = \sum \mathrm{Etot(products)} - \sum \mathrm{Etot(reactants)} \quad (1)$$

The determination of the formation enthalpy of pure $ZrNiH_3$ hydride (Eq. (3)), depends on the formation reaction (Eq. (2)):

$$ZrNiH_3(s) \leftrightarrow ZrNiH(s) + H_2(g) \quad (2)$$

$$\Delta H = \mathrm{Etot}(ZrNiH_3) - \mathrm{Etot}(ZrNiH) - \mathrm{Etot}(H_2) \quad (3)$$

As shown in Table 2, the enthalpy of formation of $ZrNiH_3$ is found equal to −67.7 kJ/mol.H_2, which is in good agreement with the experimental value of −68.8 kJ/mol.H_2 as reported by Dantzer P. et al. and Luo W et al. [31,32]. Also, this value is close to the theoretical value of - 78.029 kJ/mol.H_2 obtained previously by the authors using wien2K code [34] as well as other calculations reported in the literature reporting - 85.78 kJ/mol.H_2 [25] and −78.25 kJ/mol.H_2 [26]. The observed difference in the above values arises explicitly from the adopted approximations and codes based on DFT approaches.

Table 2 – Formation enthalpy and desorption temperature of $Zr_{1-x}TM_xNiH_3$ (TM = V, Ti, Fe, Mn, and Cr).

System	Enthalpy of formation (kJ/mol.H_2)		Desorption temperature (K)		Fermi level E_F (eV)
	Our Calculation	Experimental	Our Calculation	Experimental	
$ZrNiH_3$	−67.736	−68.6 [31,32]	521.046	547 [33]	13.9736
$Zr_{0.75}V_{0.25}NiH_3$	−53.606		412.358		14.2803
$Zr_{0.5}V_{0.5}NiH_3$	−40.960		315.083		14.4032
$Zr_{0.75}Ti_{0.25}NiH_3$	−62.902	−63.2 to −67.8 [33]	483.869	463 to 497 [33]	14.0106
$Zr_{0.5}Ti_{0.5}NiH_3$	−58.942	−55.2 to −59.2 [33]	453.403	414 to 444 [33]	13.8599
$Zr_{0.75}Fe_{0.25}NiH_3$	−49.254		378.879		14.2546
$Zr_{0.5}Fe_{0.5}NiH_3$	−26.953		207.337		14.3733
$Zr_{0.75}Mn_{0.25}NiH_3$	−46.165		355.122		14.3513
$Zr_{0.5}Mn_{0.5}NiH_3$	−27.917		214.747		14.5000
$Zr_{0.75}Cr_{0.25}NiH_3$	−48.490		373.003		14.3569
$Zr_{0.5}Cr_{0.5}NiH_3$	−31.884		245.264		14.5297

Despite our results revealed interesting and promising, they do not fully satisfy the solid storage condition that meet the US-DoE criteria [42]. For this reason, further theoretical investigations of the thermodynamic properties have been carried out. In order to reduce the stability of $ZrNiH_3$ hydride, 25% and 50% Zr has been substituted by another transition metal such as V, Ti, Fe, Mn, and Cr, which are well known for their destabilizing role in metal hydrides [43,44].

The formation reaction (Eq. (4)) of $Zr_{1-x}TM_xNiH_3$ (TM = V, Ti, Fe, Mn, and Cr, x = 0.25 and 0.50) is considered and the formation enthalpy is calculated according to Eq. (5):

$$Zr_{1-x}TM_xNiH_3(s) \leftrightarrow Zr_{1-x}TM_xNiH(s) + H_2(g) \quad (4)$$

$$\Delta H = Etot(Zr_{1-x}TM_xNiH_3) - Etot(Zr_{1-x}TM_xNiH) - Etot(H_2) \quad (5)$$

This study indicates that both the nature of the transition metal and its content within $ZrNiH_3$ decreases the formation enthalpy linearly with a specific slope for each element, thereby resulting in the enhancement of the dehydrogenation kinetics (see Fig. 4). The stability decreases in the following order: Ti > V > Fe > Cr > Mn for the content of 25% then changes to: Ti > V > Cr > Mn > Fe for the higher content of 50%.

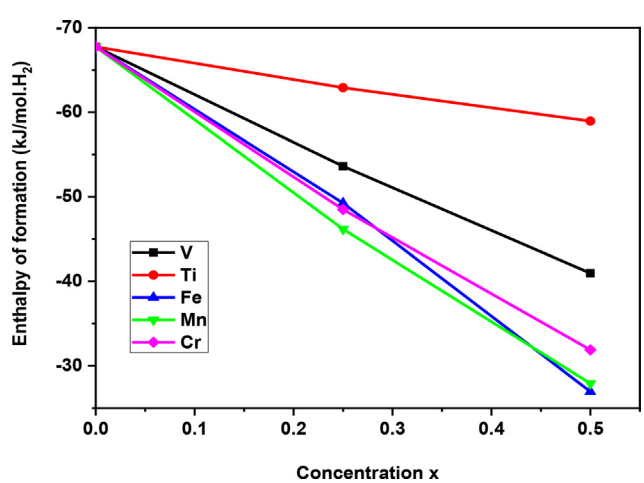

Fig. 4 – Desorption enthalpy of $Zr_{1-x}TM_xNiH_3$ according to the content x of substitution.

This statement corroborates well with the results obtained experimentally for $ZrNiH_3$ substituted with Ti from the work of Matsuyama et al. [33]. However, its stability remains high even with a content of 50% to be used as hydrogen storage material.

The linear variation in the enthalpy of formation as a function of the transition metal content is described according to Eq. (6). The specific slope for each element is given in Table 3:

$$\Delta H = \Delta H(ZrNiH_3) + Slope \times x \quad (6)$$

For optimum use of hydrogen, it is recommended to select a material with an enthalpy of a formation having a value around −40 kJ/mol.H_2 [45,46]. By introducing this value into Eq. (6) and using the calculated slope values, the content of each element resulting in the optimum value of the enthalpy of formation can be determined. Accordingly, it is found that Mn and Fe exhibit the lowest content to obtain the optimum heat of formation, which means lower stability of the substituted hydride.

Desorption temperature

The dehydrogenation temperature is given by [47–49]:

$$T_{des} = \Delta H / \Delta S \quad (7)$$

Where ΔH and ΔS represent the enthalpy of formation and the entropy of the dehydrogenation reaction. For most conventional metal hydrides, the entropy value is within the range of 95 J/K.mol < ΔS < 140 J/K.mol [50]. In the standard conditions of pressure and temperature, ΔS is found equal to 130 J/mol.K [51], which corresponds to the variation of entropy to transform 1 mol of hydrogen from the gaseous state to the solid state.

Table 3 – Content x (%) and gravimetric capacity corresponding to ΔH = −40 kJ/mol.H_2.

Systems	Slope (kJ/mol.H_2)	Content x (%)	Cg (wt.%)
$Zr_{1-x}V_xNiH_3$	53.550	51.333	2.268
$Zr_{1-x}Fe_xNiH_3$	81.564	34.784	2.150
$Zr_{1-x}Mn_xNiH_3$	79.638	34.131	2.172
$Zr_{1-x}Cr_xNiH_3$	71.703	38.062	2.167

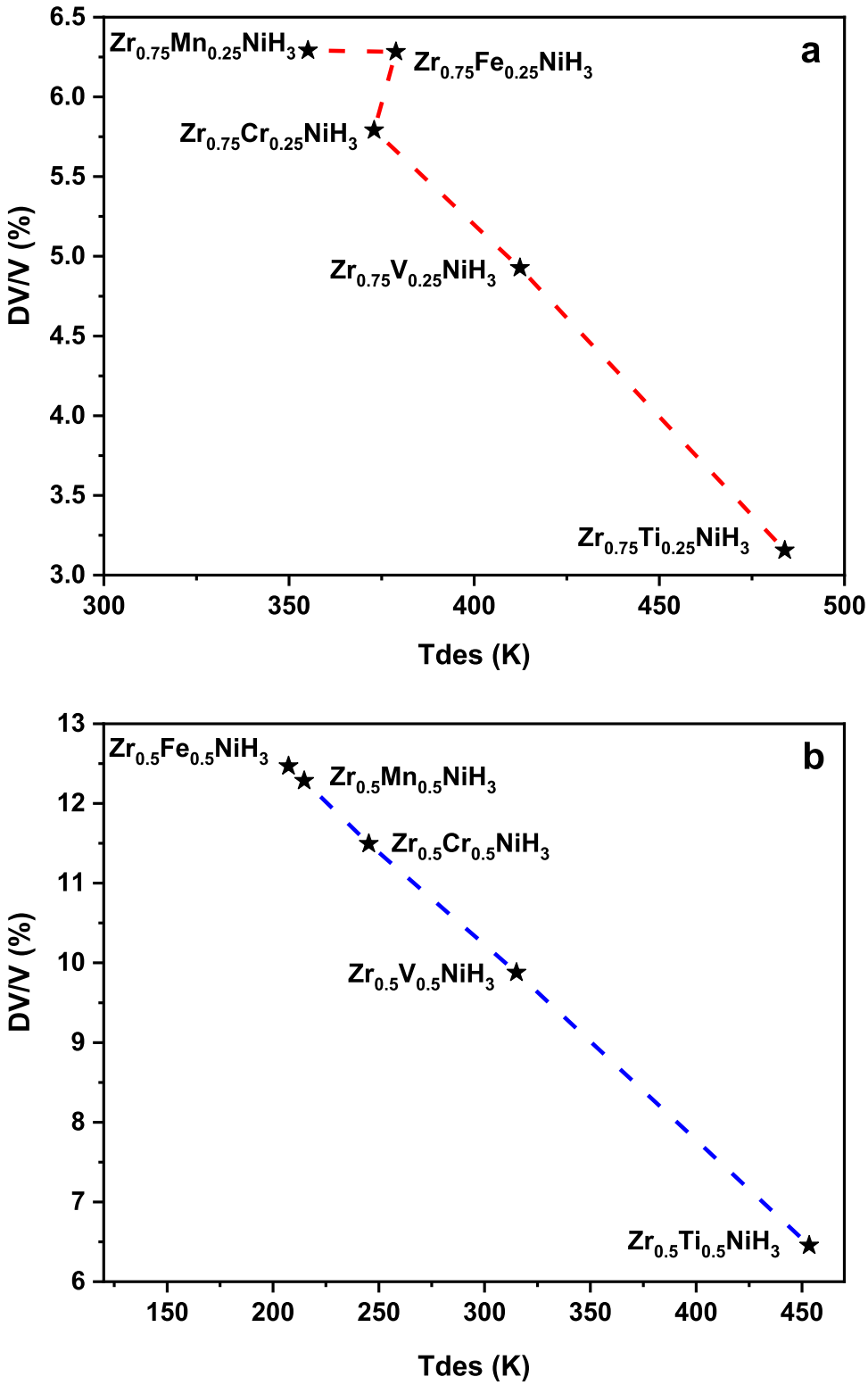

Fig. 5 – Variation of the volume as function of desorption temperature of (a) $Zr_{0.75}TM_{0.25}NiH_3$ and (b) $Zr_{0.5}TM_{0.5}NiH_3$.

Using Eq. (7) and the calculated enthalpy of formation (see Table 2) as well as the value of the entropy 130 J/mol.K, the decomposition temperature can be estimated. For pure $ZrNiH_3$, the predicted decomposition temperature is found equal to 521 K, which is very close to the reported experimental value of 547 K [33]. However, this value remains high for practical applications. Meanwhile, as mentioned earlier, the replacement of Zr by 25 and 50% of transition metals have

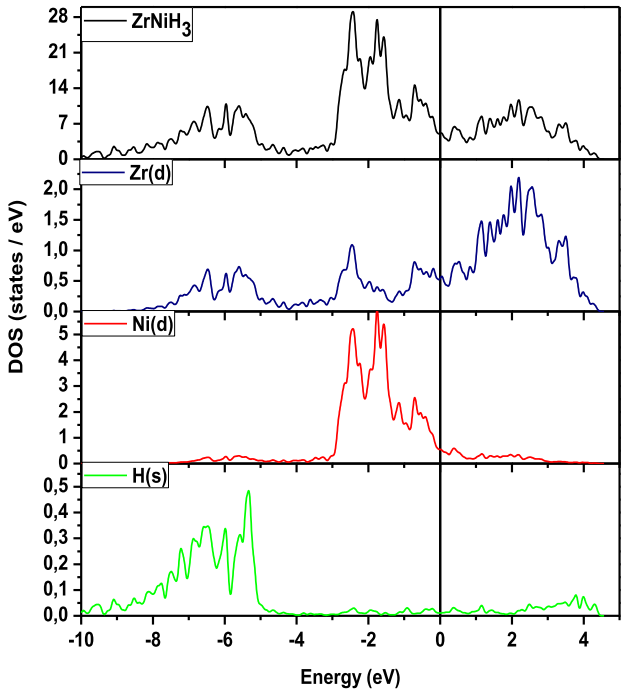

Fig. 6 – Total and partial DOS of pure $ZrNiH_3$.

a significant effect on the destabilization of the hydride and consequently, the achieved decrease in the decomposition temperature is found in the same order obtained for the enthalpy of formation. In addition, it is observed that the desorption temperature decreases as a function of the volume change of the compounds (ΔV/V in %) (see Fig. 5), which means that more the hydride is stable, more the variation of the volume of the compound is low.

It can be concluded that these compounds $Zr_{1-x}TM_xNiH_3$ (with TM = V, Fe, Mn and Cr) with the content cited in Table 3, will satisfy several criteria for hydrogen storage in solid-state: (i) stability - 40 kJ/mol.H_2; (ii) decomposition temperature in the range 233–358 K and volumetric capacity of 30–50 g.H_2/l for practical use as advised recently by the U.S. Department of Energy (DOE) for stability and volumetric capacity criteria [42]. Hence, it can be considered as a promising material for hydrogen storage, except its gravimetric capacity remaining relatively low; i.e. 2.3 wt%. Nevertheless, this hydride is very suitable for applications where the gravimetric capacity is not a priority constraint, such as stationary applications and as negative electrode active material for the nickel metal hydride (Ni-MH) rechargeable batteries [30, 52, 53].

Electronic structure

The density of state as a function of energy has been used to study and explain the influence of substituting Zr by another transition metal on both stability and desorption temperature of the $ZrNiH_3$ compound. For this purpose, the total (DOS) and partial densities (PDOS) are calculated and plotted in Figs. 6–11. The Fermi level (E_F) is set to zero and used as a reference (the computed values of the real Fermi level (E_F) for each hydride are reported in Table 2).

From Fig. 6, it can be deduced that $ZrNiH_3$ has a metallic character. The contribution of the conduction band is fully from Zr–d with a small contribution arising from Ni–d states. While, in the valence band, there are two parts. The first part concerns the band with energy from −3 to 0.0 eV (high energy

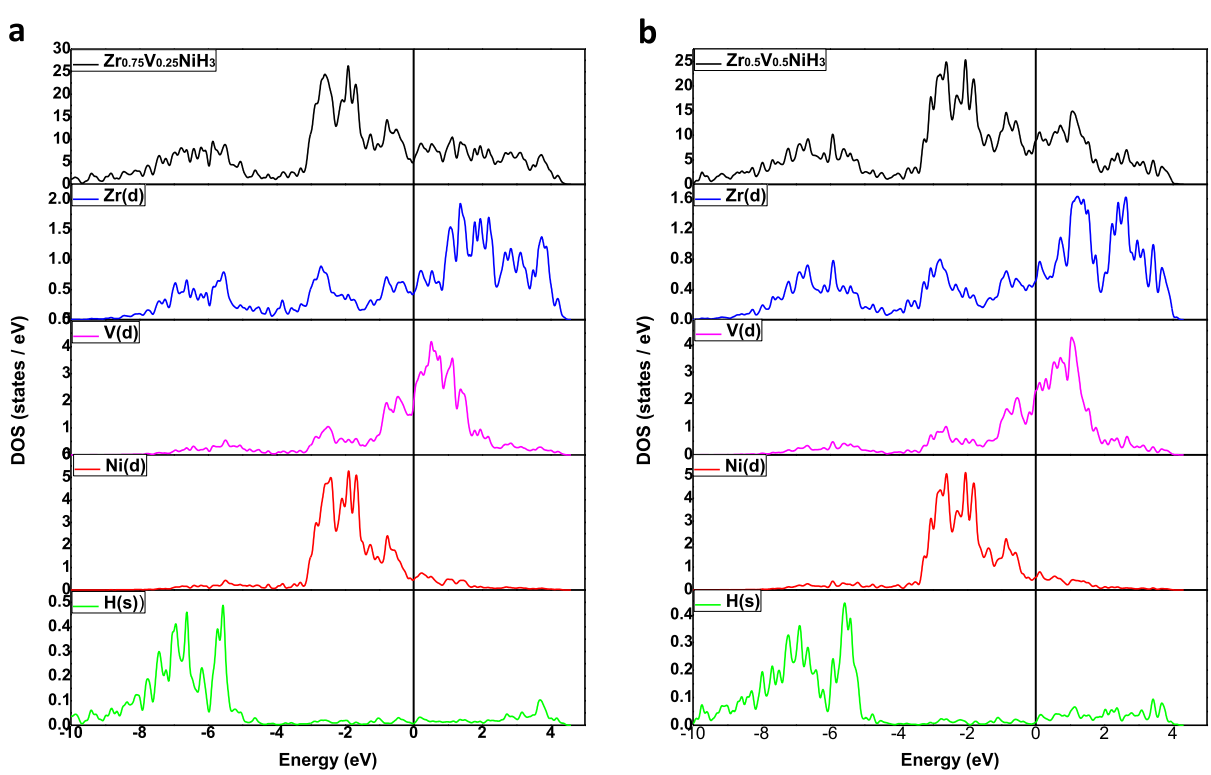

Fig. 7 – Total and partial DOS of (a) $Zr_{0.75}V_{0.5}NiH_3$ and (b) $Zr_{0.5}V_{0.5}NiH_3$.

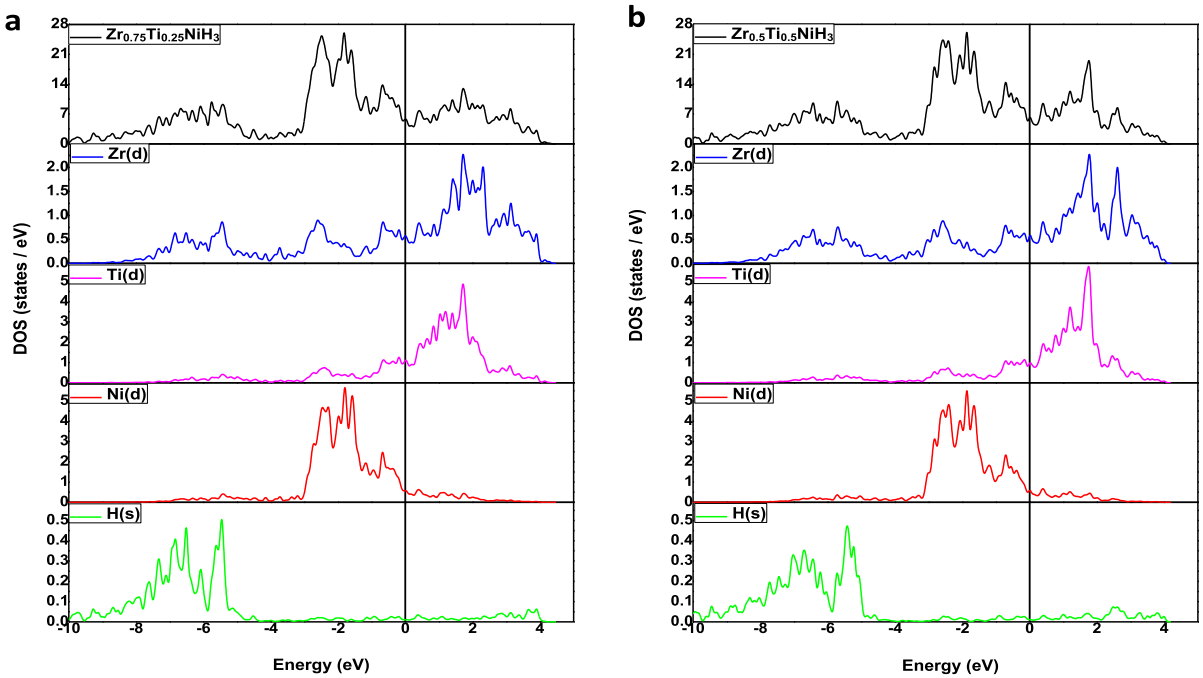

Fig. 8 – Total and partial DOS of (a) $Zr_{0.75}Ti_{0.5}NiH_3$ and (b) $Zr_{0.5}Ti_{0.5}NiH_3$.

states), which is composed almost from Ni-d states. The second range covers the band with energy from −9 to −4 eV (low energy states), originating mainly from Zr-d and H-s states. The formation of the metal-hydrogen bonding in the $ZrNiH_3$ compound results from a strong hybridization between the H-s, Zr-d, and Ni-d states. This observation may explain the high stability and high decomposition temperature obtained earlier.

For $ZrNiH_3$ substituted with transition metals TM (TM = V, Ti, Fe, Mn, and Cr) (see Figs. 7–11), both DOS and PDOS indicate that the overall shapes of the electronic structure are similar to each other, signifying that the system preserves the same electronic behavior as observed in $ZrNiH_3$.

For example, in Fig. 7 the main contribution to the total and partial DOS of $Zr_{0.75}V_{0.5}NiH_3$ and $Zr_{0.5}V_{0.5}NiH_3$ arises from the d state of transition metal TM, which indicates that there is a weak hybridization between TM-d and H-s unlike pure $ZrNiH_3$, where a strong hybridization between the H and transition metals (Zr and Ni) atoms occurs. The valence band is divided into two parts: (i) the first part with an energy

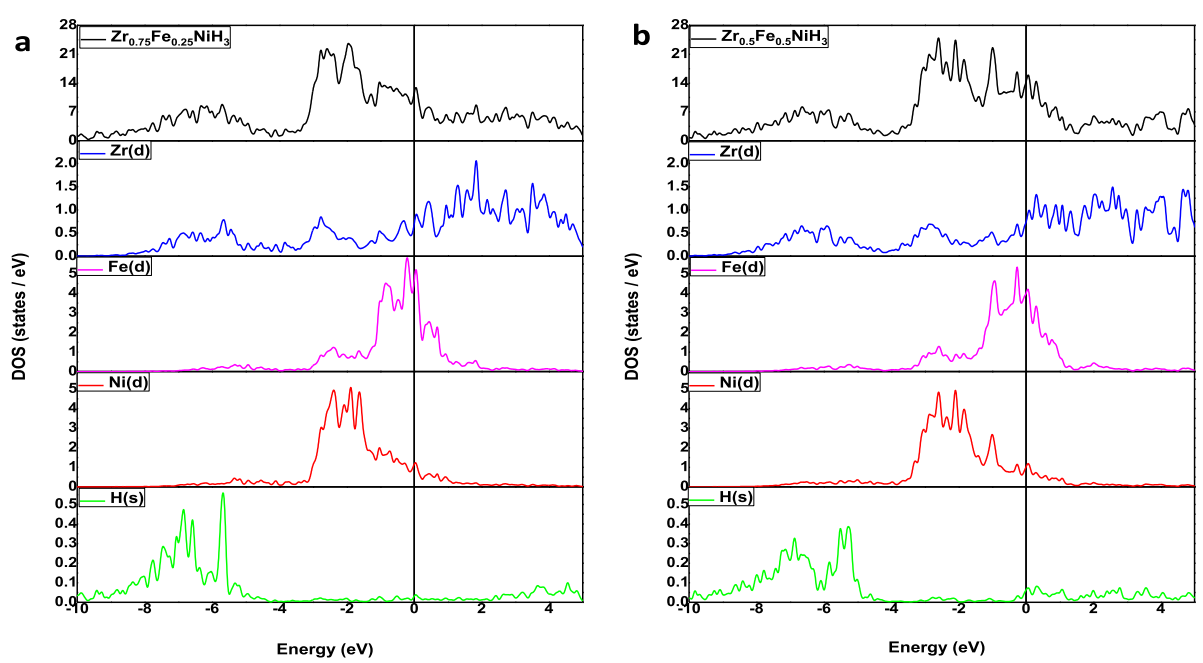

Fig. 9 – Total and partial DOS of (a) $Zr_{0.75}Fe_{0.5}NiH_3$ and (b) $Zr_{0.5}Fe_{0.5}NiH_3$.

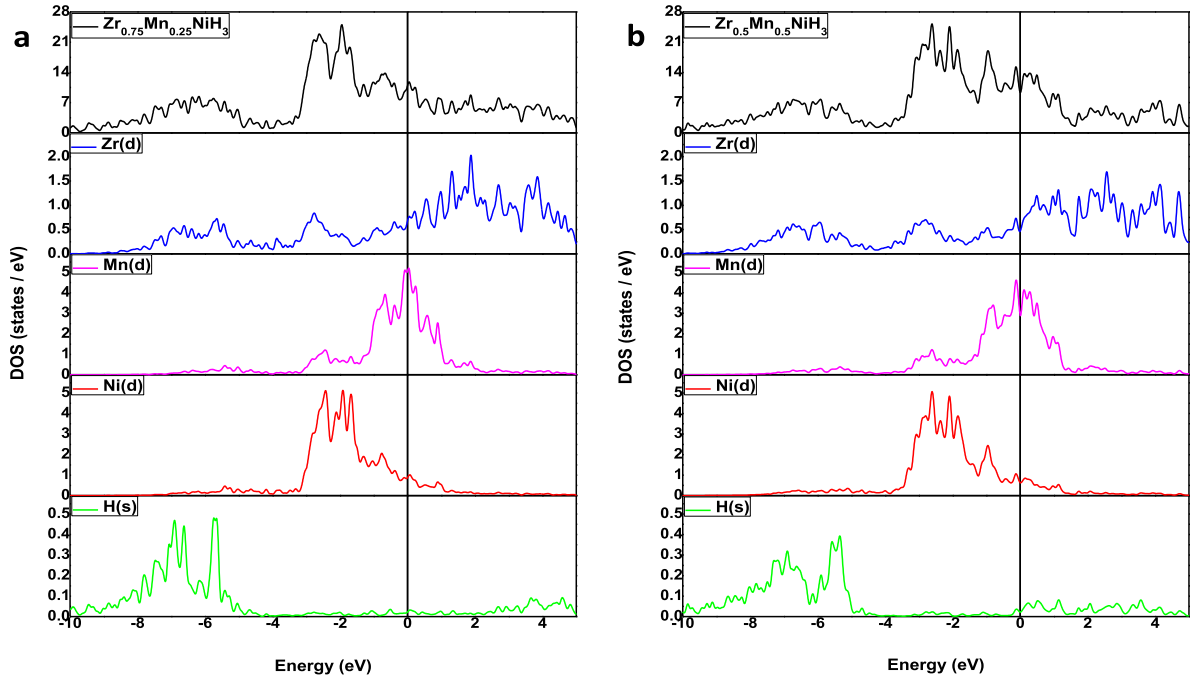

Fig. 10 – Total and partial DOS of (a) $Zr_{0.75}Mn_{0.5}NiH_3$ and (b) $Zr_{0.5}Mn_{0.5}NiH_3$.

ranging from −9 to −4 eV (low energy states) originating mainly from Zr-d and H-1s orbitals and presents a weak hybridization between Ni-d and H-s states; (ii) the second part from −4.0 to 0 eV (high energy states) consists of Ni-d and TM-d orbitals, indicating a high hybridization near to the Fermi level. Beyond the Fermi level, the DOS is dominated by TM and Zr d states.

The same features are observed for other elements Ti, Fe, Mn, and Cr. The only small difference between different components is observed in the d states of transition metals TM (T i, V, Fe and Ni) which is localized in the band gap according to the following order:

Ti → V → Cr → Fe → Mn.

From the obtained DOS and PDOS results, it is evident that the substitution of Zr by transition metals TM (TM = V, Ti, Fe, Mn, and Cr) into the intermetallic hydride $ZrNiH_3$, can efficiently reduce the interactions between the interstitial H and

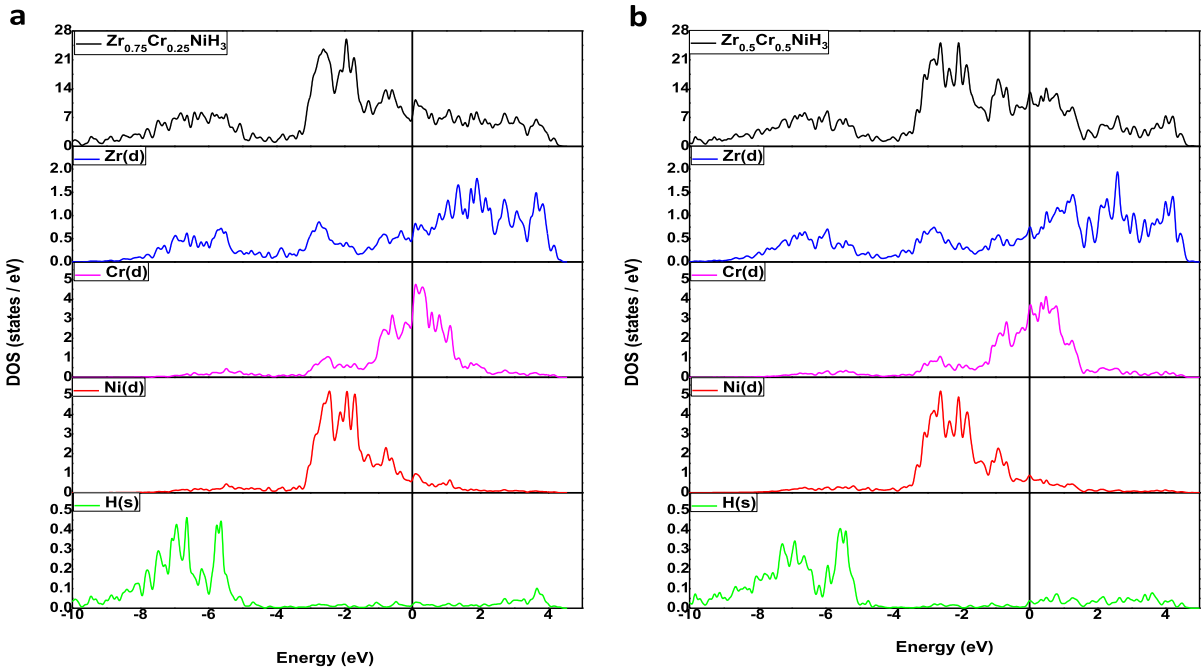

Fig. 11 – Total and partial DOS of (a) $Zr_{0.75}Cr_{0.5}NiH_3$ and (b) $Zr_{0.5}Cr_{0.5}NiH_3$.

both Zr and Ni host. This ascertainment agrees with the results obtained for the enthalpy of formation, where the incorporation of the transition elements in $ZrNiH_3$ decreases simultaneously the stability and the desorption temperature.

Conclusion

In this paper, first-principles calculations were performed to investigate the hydrogen storage properties of the intermetallic hydride $Zr_{1-x}TM_xNiH_3$ (x = 0.25, 0.50; TM = V, Ti, Fe, Mn, and Cr). It was found that the substitution of Zr by another transition metal could extremely decrease the stability of the ternary hydride, the decomposition temperature, and accelerate the kinetics of desorption without reducing its gravimetric and volumetric capacities. The analysis of the density of states of $Zr_{1-x}TM_xNiH_3$ showed that the main contribution to the total DOS originates from the d state of transition metals, meanwhile the electronic behavior for each system was preserved. There was a weak hybridization between TM-d and H-s, unlike pure $ZrNiH_3$, where a strong hybridization occurred between these states. It was noted that $ZrNiH_3$ substituted with Fe and Mn exhibited the highest density of state near the Fermi level. Thus, it was worthwhile to note that this theoretical study predicted that, particularly, Mn and Fe substituted $ZrNiH_3$ resulted in better dehydrogenation proprieties compared to that obtained experimentally for Ti substituted $ZrNiH_3$

Declaration of competing interest

The authors declare that they have no known competing financial interests or personal relationships that could have appeared to influence the work reported in this paper.

REFERENCES

[1] Züttel A, Remhof A, Borgschulte A, Friedrichs O. Hydrogen: the future energy carrier. Proc R Soc A 2010;368:3329–42. https://doi.org/10.1098/rsta.2010.0113.

[2] Rusman NAA, Dahari M. A review on the current progress of metal hydrides material for solid-state hydrogen storage applications. Int J Hydrogen Energy 2016;41:12108–26. https://doi.org/10.1016/j.ijhydene.2016.05.244.

[3] Bellosta von Colbe J, Ares J-R, Barale J, Baricco M, Buckley C, Capurso G, et al. Application of hydrides in hydrogen storage and compression: achievements, outlook and perspectives. Int J Hydrogen Energy 2019;44:7780–808. https://doi.org/10.1016/j.ijhydene.2019.01.104.

[4] Dagdougui H, Sacile R, Bersani C, Ouammi A. Hydrogen storage and distribution: implementation scenarios. Hydrogen infrastructure for energy applications. Elsevier; 2018. p. 37–52. https://doi.org/10.1016/B978-0-12-812036-1.00004-4.

[5] Moradi R, Groth KM. Hydrogen storage and delivery: review of the state of the art technologies and risk and reliability analysis. Int J Hydrogen Energy 2019;44:12254–69. https://doi.org/10.1016/j.ijhydene.2019.03.041.

[6] Alaoui-Belghiti A, Rkhis M, Laasri S, Hajjaji A, Eljouad M, EL-Otmani R, et al. Conception and numerical simulation of heat and mass transfer in a solid state hydrogen storage reactor. Eur Phys J Appl Phys 2019;87:20902. https://doi.org/10.1051/epjap/2019190087.

[7] Schlapbach L, Züttel A. Hydrogen-storage materials for mobile applications. Nature 2001;414:353–8. https://doi.org/10.1038/35104634.

[8] Liu Y, Pan H. Hydrogen storage materials. New and Future Developments in Catalysis 2013:377–405. https://doi.org/10.1016/B978-0-444-53880-2.00018-1.

[9] Zhang Q, Zang L, Huang Y, Gao P, Jiao L, Yuan H, et al. Improved hydrogen storage properties of MgH_2 with Ni-based compounds. Int J Hydrogen Energy 2017;42:24247–55. https://doi.org/10.1016/j.ijhydene.2017.07.220.

[10] Drulis H, Hackemer A, Folcik L, Giza K, Bala H, Gondek Ł, et al. Thermodynamic and electrochemical hydrogenation properties of $LaNi_{5-x}In_x$ alloys. Int J Hydrogen Energy 2012;37:15850–4. https://doi.org/10.1016/j.ijhydene.2012.08.010.

[11] Zhou W, Zhu D, Liu K, Li J, Wu C, Chen Y. Long-life Ni-MH batteries with high-power delivery at lower temperatures: coordination of low-temperature and high-power delivery with cycling life of low-Al AB_5-type hydrogen storage alloys. Int J Hydrogen Energy 2018;43:21464–77. https://doi.org/10.1016/j.ijhydene.2018.09.166.

[12] Uesato H, Miyaoka H, Ichikawa T, Kojima Y. Hybrid nickel-metal hydride/hydrogen battery. Int J Hydrogen Energy 2019;44:4263–70. https://doi.org/10.1016/j.ijhydene.2018.12.114.

[13] Cao Z, Ouyang L, Li L, Lu Y, Wang H, Liu J, et al. Enhanced discharge capacity and cycling properties in high-samarium, praseodymium/neodymium-free, and low-cobalt A 2 B 7 electrode materials for nickel-metal hydride battery. Int J Hydrogen Energy 2015;40:451–5. https://doi.org/10.1016/j.ijhydene.2014.11.016.

[14] Bäuerlein P, Antonius C, Löffler J, Kümpers J. Progress in high-power nickel–metal hydride batteries. J Power Sources 2008;176:547–54. https://doi.org/10.1016/j.jpowsour.2007.08.052.

[15] Zhao X, Ma L. Recent progress in hydrogen storage alloys for nickel/metal hydride secondary batteries. Int J Hydrogen Energy 2009;34:4788–96. https://doi.org/10.1016/j.ijhydene.2009.03.023.

[16] Feng F. Electrochemical behaviour of intermetallic-based metal hydrides used in Ni/metal hydride (MH) batteries: a review. Int J Hydrogen Energy 2001;26:725–34. https://doi.org/10.1016/S0360-3199(00)00127-0.

[17] Larsson F, Andersson P, Blomqvist P, Lorén A, Mellander B-E. Characteristics of lithium-ion batteries during fire tests. J Power Sources 2014;271:414–20. https://doi.org/10.1016/j.jpowsour.2014.08.027.

[18] Larsson F, Andersson P, Mellander B-E. Lithium-ion battery aspects on fires in electrified vehicles on the basis of experimental abuse tests. Batteries 2016;2:9. https://doi.org/10.3390/batteries2020009.

[19] Korst WL. The crystal structure of $NiZrH_3$. J Phys Chem 1962;66(2):370–2. https://doi.org/10.1021/j100808a515.

[20] Peterson SW, Sadana VN, Korst WL. Neutron diffraction study of nickel zirconium hydride. J Phys France 1964;25:451–3. https://doi.org/10.1051/jphys:01964002505045100.

[21] Westlake DG, Shaked H, Mason PR, McCart BR, Mueller MH, Matsumoto T, et al. Interstitial site occupation in ZrNiH. J Less Common Met 1982;88:17–23. https://doi.org/10.1016/0022-5088(82)90005-4.

[22] Westlake DG. Stoichiometries and interstitial site occupation in the hydrides of zrni and other isostructural intermetallic compounds. J Less-Common Met 1980;75(2):177–85. https://doi.org/10.1016/0022-5088(80)90115-0.

[23] Varga LK, Tompa K, Lovas A, Joubert JM, Percheron-Guegant A. Maximum hydrogen storage capacity of amorphous $Ni_{1-x}Zr_x$ alloys. Int J Hydrogen Energy 1996;21:927–30.

[24] Simonovic B. Multiple hydriding/dehydriding of $Zr_{1.02}Ni_{0.98}$ alloy. Int J Hydrogen Energy 1999;24:449–54. https://doi.org/10.1016/S0360-3199(98)00090-1.

[25] Bouhadda Y, Rabehi A, Boudouma Y, Fenineche N, Drablia S, Meradji H. Hydrogen solid storage: first-principles study of $ZrNiH_3$. Int J Hydrogen Energy 2009;34:4997–5002. https://doi.org/10.1016/j.ijhydene.2008.12.082.

[26] Chattaraj D, Dash S, Majumder C. Structural, electronic, elastic, vibrational and thermodynamic properties of ZrNi and $ZrNiH_3$: a comprehensive study through first principles approach. Int J Hydrogen Energy 2016;41:20250–60. https://doi.org/10.1016/j.ijhydene.2016.09.046.

[27] Nakano H, Wakao S. Substitution effect of elements in Zr-based alloys with Laves phase for nickel-hydride battery. J Alloys Compd 1995;231:587–93. https://doi.org/10.1016/0925-8388(95)01733-X.

[28] Khaldi C. Electrochemical study of cobalt-free AB_5-type hydrogen storage alloys. Int J Hydrogen Energy 2004;29:307–11. https://doi.org/10.1016/S0360-3199(03)00157-5.

[29] Zhu Y, Pan H, Gao M, Ma J, Lei Y, Wang Q. Electrochemical studies on the Ti-Zr-V-Mn-Cr-Ni hydrogen storage electrode alloys. Int J Hydrogen Energy 2003;28:311–6. https://doi.org/10.1016/S0360-3199(02)00083-6.

[30] Matsuyama A, Mizutani H, Kozuka T, Inoue H. Effect of surface treatment with boiling alkaline solution on electrochemical properties of the ZrNi alloy electrode. Int J Hydrogen Energy 2016;41:9908–13. https://doi.org/10.1016/j.ijhydene.2016.01.033.

[31] Dantzer P, Millet P, Flanagan TB. Thermodynamic characterization of hydride phase growth in ZrNi-H_2. Metall Mater Trans 2001;32:29–38. https://doi.org/10.1007/s11661-001-0248-x.

[32] Luo W, Craft A, Kuji T, Chung HS, Flanagan TB. Thermodynamic characterization of the ZrNi-H system by reaction calorimetry and p-c-t measurements. J Less Common Met 1990;162:251–66. https://doi.org/10.1016/0022-5088(90)90341-G.

[33] Matsuyama A, Mizutani H, Kozuka T, Inoue H. Crystal structure and hydrogen absorption-desorption properties of $Zr_{1-x}Ti_xNi$ ($0.05 \leq x \leq 0.5$) alloys. J Alloys Compd 2017;714:467–75. https://doi.org/10.1016/j.jallcom.2017.04.217.

[34] Rkhis M, Alaoui-Belghiti A, Laasri S, Touhtouh S, Hajjaji A, Hlil EK, et al. First principle investigation on hydrogen solid storage in $Zr_{1-x}Nb_xNiH_3$ ($x = 0$ and 0.1). Int J Hydrogen Energy 2019;44:23188–95. https://doi.org/10.1016/j.ijhydene.2019.07.017.

[35] Bickelhaupt FM, Baerends EJ. Kohn-Sham density functional theory: predicting and understanding chemistry. In: Lipkowitz KB, Boyd DB, editors. Reviews in computational chemistry. Hoboken, NJ, USA: John Wiley & Sons, Inc.; 2007. p. 1–86. https://doi.org/10.1002/9780470125922.ch1.

[36] Giannozzi P, Baroni S, Bonini N, Calandra M, Car R, Cavazzoni C, et al. Quantum espresso: a modular and open-source software project for quantum simulations of materials. J Phys Condens Matter 2009;21:395502. https://doi.org/10.1088/0953-8984/21/39/395502.

[37] Perdew JP, Burke K, Ernzerhof M. Generalized gradient approximation made simple. Phys Rev Lett 1996;77:3865–8. https://doi.org/10.1103/PhysRevLett.77.3865.

[38] Vanderbilt D. Soft self-consistent pseudopotentials in a generalized eigenvalue formalism. Phys Rev B 1990;41:7892–5. https://doi.org/10.1103/PhysRevB.41.7892.

[39] Feynman RP. Forces in molecules. Phys Rev 1939;56:340–3. https://doi.org/10.1103/PhysRev.56.340.

[40] Yang S, Aubertin F, Rehbein P, Gonser U. A Mossbauer spectroscopy study of the system ZrNi-H and ZrCo-H. Zeitschrift Fur Kristallagraphie 1991;195(3–4):281–92. https://doi.org/10.1524/zkri.1991.195.3-4.281.

[41] Denton AR, Ashcroft NW. Vegard's law. Phys Rev A 1991;43:3161–4. https://doi.org/10.1103/PhysRevA.43.3161.

[42] Abe JO, Popoola API, Ajenifuja E, Popoola OM. Hydrogen energy, economy and storage: review and recommendation. Int J Hydrogen Energy 2019;44:15072–86. https://doi.org/10.1016/j.ijhydene.2019.04.068.

[43] Shang C. Mechanical alloying and electronic simulations of (MgH_2+M) systems (M=Al, Ti, Fe, Ni, Cu and Nb) for hydrogen storage. Int J Hydrogen Energy 2004;29:73–80. https://doi.org/10.1016/S0360-3199(03)00045-4.

[44] Novaković N, Grbović Novaković J, Matović L, Manasijević M, Radisavljević I, Paskaš Mamula B, et al. Ab initio calculations of MgH_2, MgH_2:Ti and MgH_2:Co compounds. Int J Hydrogen Energy 2010;35:598–608. https://doi.org/10.1016/j.ijhydene.2009.11.003.

[45] Gremaud R, Broedersz CP, Borsa DM, Borgschulte A, Mauron P, Schreuders H, et al. Hydrogenography: an optical combinatorial method to find new light-weight hydrogen-storage materials. Adv Mater 2007;19:2813–7. https://doi.org/10.1002/adma.200602560.

[46] Klebanoff LE, Keller JO. 5 Years of hydrogen storage research in the U.S. DOE metal hydride center of excellence (MHCoE). Int J Hydrogen Energy 2013;38:4533–76. https://doi.org/10.1016/j.ijhydene.2013.01.051.

[47] EL Kassaoui M, Lakhal M, Abdellaoui M, Benyoussef A, El Kenz A, Loulidi M. Modeling hydrogen adsorption in the metal organic framework (MOF-5, connector): $Zn_4O(C_8H_4O_4)_3$. Int J Hydrogen Energy 2020. https://doi.org/10.1016/j.ijhydene.2020.03.168. S0360319920311794.

[48] Bahou S, Labrim H, Lakhal M, Bhihi M, Hartiti B, Ez-Zahraouy H. Improving desorption temperature and kinetic properties in MgH_2 by vacancy defects: DFT study. Int J Hydrogen Energy 2020;45:10806–13. https://doi.org/10.1016/j.ijhydene.2020.02.024.

[49] Garara M, Benzidi H, Lakhal M, Louilidi M, Ez-Zahraouy H, El Kenz A, et al. Phosphorene: a promising candidate for H_2 storage at room temperature. Int J Hydrogen Energy 2019;44:24829–38. https://doi.org/10.1016/j.ijhydene.2019.07.194.

[50] Alapati SV, Johnson JK, Sholl DS. Identification of destabilized metal hydrides for hydrogen storage using first principles calculations. J Phys Chem B 2006;110:8769–76. https://doi.org/10.1021/jp060482m.

[51] Zeng Q, Su K, Zhang L, Xu Y, Cheng L, Yan X. Evaluation of the thermodynamic data of CH_3SiCl_3 based on quantum chemistry calculations. J Phys Chem Ref Data 2006;35:1385–90. https://doi.org/10.1063/1.2201867.

[52] Matsuyama A, Mizutani H, Kozuka T, Inoue H. Effect of Ti substitution on electrochemical properties of ZrNi alloy electrode for use in nickel-metal hydride batteries. Int J Hydrogen Energy 2017;42:22622–7. https://doi.org/10.1016/j.ijhydene.2017.03.119.

[53] Lai Q, Paskevicius M, Sheppard DA, Buckley CE, Thornton AW, Hill MR, et al. Hydrogen storage materials for mobile and stationary applications: current state of the art. ChemSusChem 2015;8:2789–825. https://doi.org/10.1002/cssc.201500231.